

# Investigation on Energy Director-less Ultrasonic Welding of Polyetherimide (PEI)- to Epoxy-based Composites

Eirini Tsiangou<sup>a,\*</sup>, Sofia Teixeira de Freitas<sup>a</sup>, Irene Fernandez Villegas<sup>a</sup>, Rinze Benedictus<sup>a</sup>

<sup>a</sup> Aerospace Structures and Materials Department, Faculty of Aerospace Engineering, Delft University of Technology, Kluyverweg 1, 2629HS Delft, The Netherlands

\*Corresponding author. E-mail address: E.Tsiangou@tudelft.nl

## Abstract

In ultrasonic welding of thermoplastic composites an energy director (ED) (i.e. neat thermoplastic film), is used between the two adherends to be welded, to promote frictional and viscoelastic heating. For welding of **thermoset composites (TSC)**, a thermoplastic coupling layer is co-cured on the surface to be welded as typical procedure to make the TSC “weldable”. This study focuses on investigating whether a polyetherimide (PEI) coupling layer by itself has the potential to promote heat generation during ultrasonic welding of CF/epoxy and CF/PEI samples, without the need for a separate ED, and if so, what thickness should that coupling layer be. The main findings were that welding without a loose ED resulted in overheating of the CF/PEI adherend and/or coupling layer due to the inability of the latter to promote heat generation efficiently. However, welding of CF/epoxy and CF/PEI samples with the use of a loose ED resulted in high-strength welds.

**Keywords:** A. Polymer-matrix composites (PMCs), A. Thermoplastic resin, A. Thermosetting resin, E. Joints/joining

## 1. Introduction

Using dissimilar composite parts is becoming more popular in the aerospace industry. Two examples are the Airbus A350 and Boeing 787 passenger aircraft, in which thousands of thermoplastic composite (TPC) clips are used in the carbon fibre (CF)/epoxy fuselage. The joint between these parts is currently attained with mechanical fasteners, which are not the most

suitable for composite structures [1]. An alternative joining method is adhesive bonding. However, extensive surface preparation is necessary to create strong bonds, and in most cases, curing of the thermoset adhesive is time consuming (minimum a couple of hours) [1]. Welding, on the other hand, does not require any surface preparation and is a much faster joining process as compared to the two methods mentioned above (from a few seconds to a couple of minutes) [2,3]. In order for welding to become an alternative to mechanical fastening of dissimilar composite parts, it should be further explored and understood since only a limited number of studies can be found in literature [1,4,5]

One way to make thermoset composites (TSC) weldable is by placing a neat, compatible thermoplastic (TP) layer, hereafter called “coupling layer”, on the surface of the uncured laminate, and subsequently subjecting the stack (i.e. the adherend and the coupling layer) to a co-curing process [6]. Even though curing refers to the chemical reaction that occurs in the thermoset resin only, the term “co-curing” is used in literature to describe the process of bonding a thermoplastic film with a TSC [5]. Therefore, the same term will be used in this study for consistency. Compatibility between the coupling layer and the thermoset (TS) adherend allows for interdiffusion of the monomers of the thermoset resin into the polymer and vice versa, during the co-curing process [7]. Interdiffusion and ultimately phase separation between the thermoset and thermoplastic resins result in an interphase with gradient composition and morphology between the two materials, which is a reliable way to bond a TP layer to a TSC [7]. **Note that apart from partial solubility, compatibility between the TP and TS materials requires that the TP material has a glass transition temperature ( $T_g$ ) above the curing temperature of the TS resin.** In principle, after the co-curing process is finished, the TSC laminate can be welded through the coupling layer following any welding process.

In this study, ultrasonic welding was used to weld a TSC material to a TPC material, as it is the fastest welding method at the moment, with heating times of less than 1 s [4,8]. **As reported in a previous study [3], the short heating times of less than 500 ms,** can help prevent the epoxy matrix from thermally degrading during welding, since the time for the heat to be transferred from the weld interface to the TS component as well as for the degradation mechanisms to occur is limited.

To ensure very short heating times, a combination of high force and amplitude of the vibrations were used in that study. In the ultrasonic welding process of TPCs, a neat, flat TP resin layer (normally made of the same material as the TP matrix), referred to as energy director (ED), is placed between the two adherends to be welded. The ED is responsible for generating heat locally at the interface through preferential frictional and viscoelastic heating. Frictional heating is responsible for initiating heat generation. Viscoelastic heating becomes the dominant heating mechanism once the temperature of the resin reaches its  $T_g$  [8]. However, for welding TSCs a neat TP layer already exists, i.e. the TP coupling layer co-cured on the TSC laminate. It is unknown whether an additional ED is still needed or whether the coupling TP layer itself is sufficient to guarantee a weld with good mechanical performance. Not using an ED could make the assembly process faster by eliminating the step of fixing the ED on the surface of the adherend and result in the use of less material. On the other hand, removing the ED is expected to affect the heat generation at the interface. The coupling layer and TPC adherend will be more involved in heat generation, as compared to the case when an ED is used. Hence the coupling layer is expected to be unable to act as a thermal barrier for the TS resin and it is possible that more heat will be transferred from the coupling layer to the TSC adherend. This might subsequently result in overheating of the TSC adherend and thus poor weld quality.

The present paper aims at assessing whether it is feasible to ultrasonically weld CF/Polyetherimide (PEI) to CF/epoxy composites by using only the co-cured PEI coupling layer as an integrated ED. PEI was chosen as the material for the coupling layer as it is known to be compatible with most epoxy systems [7]. Two thicknesses were examined for the coupling layer, namely 60 and 250  $\mu\text{m}$ . The TPC adherend was made out of CF/PEI to match the material of the coupling layer. The main aspects investigated were the effect of the absence of a loose ED (hereafter referred to as ED-less process) on: (i) the welding process (e.g. the power dissipated during the process and the displacement of the sonotrode curves), (ii) the integrity of the welding stack, i.e. the adherends and the coupling layer after welding and (iii) the mechanical performance of the welded joints. The ED-less process was compared to a reference welded case, in which a loose flat PEI ED was used. The mechanical performance of the samples of all welded cases were also compared to reference co-cured samples.

## 2. Experimental Procedure

### 2.1 Materials and manufacturing

In this study, Cetex® CF/PEI powder-coated semi-preg with a 5-harness satin weave fabric, manufactured by TenCate Advanced Composites (The Netherlands) was used as the material to produce the TPC adherends. The CF/PEI laminates had a [0/90]3s stacking sequence and were consolidated in a hot-press at 320 °C and 20 bar for 30 min. The thickness of the consolidated laminates was around 2 mm.

As the TSC material, T800S/3911 unidirectional CF/epoxy prepreg from TORAY (Japan) was used. Unidirectional CF/epoxy pre-preg was manually stacked in a [0,90]2s configuration. A neat PEI film was placed on one of the sides of the CF/epoxy laminates, serving as the coupling layer. Two PEI coupling layers with two different thicknesses were used, a 60 µm-thick PEI film provided by SABIC (The Netherlands), and a 250 µm-thick PEI film provided by LITE (Germany). The PEI coupling layer was degreased with isopropanol prior to its application on top of the CF/epoxy prepreg stack. The coupling layer was kept in place because of the tackiness of the uncured epoxy resin. The CF/epoxy laminates with the attached coupling layer were cured in an autoclave at 180°C and 7 bars for 120 min, according to the specifications of the manufacturer. A Wrightlon® 7400 nylon foil provided by MCTechnics was used as the material of the vacuum bag. To ensure flat surfaces on both sides of the CF/epoxy laminate, an aluminium caul plate was used on the side of the vacuum bag and on the opposite side a standard aluminium flat mould. The thickness of the CF/epoxy/PEI cured laminates was 1.9 mm for the 60 µm coupling layer and 2.28 mm for the 250 µm one. Even though extensive work has been published on the miscibility of epoxy and PEI resins [5,7,9], the combination of the T800S/3911 and PEI materials has not been reported yet in literature. Hence, an investigation on whether an interphase was formed between the two abovementioned materials was conducted and it is presented in the baseline study of the results section. Finally, the material of the ED was the same as the 250 µm-thick PEI coupling layer.

The CF/PEI and CF/epoxy/PEI adherends with dimensions 25.4 mm x 101.6 mm were cut from the laminates using a water-cooled circular diamond saw. The CF/PEI adherends were cut with their longitudinal direction parallel to the main apparent orientation of the fibres. The CF/epoxy/PEI adherends were cut with their longitudinal direction parallel to the 0° fibres.

CF/epoxy laminates directly co-cured with CF/PEI laminates were manufactured as co-cured reference specimens. **Note that, in this case, a neat PEI film was not used on top of the CF/epoxy laminate, because at 180 °C the PEI resin is still in solid state, hence it cannot adhere to the CF/PEI adherend.** An uncured CF/epoxy prepreg stack and a consolidated CF/PEI laminate were first cut in 200 mm-length and 200 mm-width and then stacked. In order to produce samples with a single-lap configuration, two release films were placed between the uncured CF/epoxy and the CF/PEI laminates with a gap of 12.7 mm, as seen in Figure 1a. Afterwards, the stack was co-cured following the same autoclave cycle mentioned above for the CF/epoxy laminate. The release films allowed for the two materials to be co-cured only at the desired location. Subsequent to the co-curing process, the parts indicated with the diagonal lines in Figure 1a were cut out, in order to produce the single-lap specimens. Finally, the individual specimens were cut in 25.4 mm-width dimension, as seen in Figure 1b.

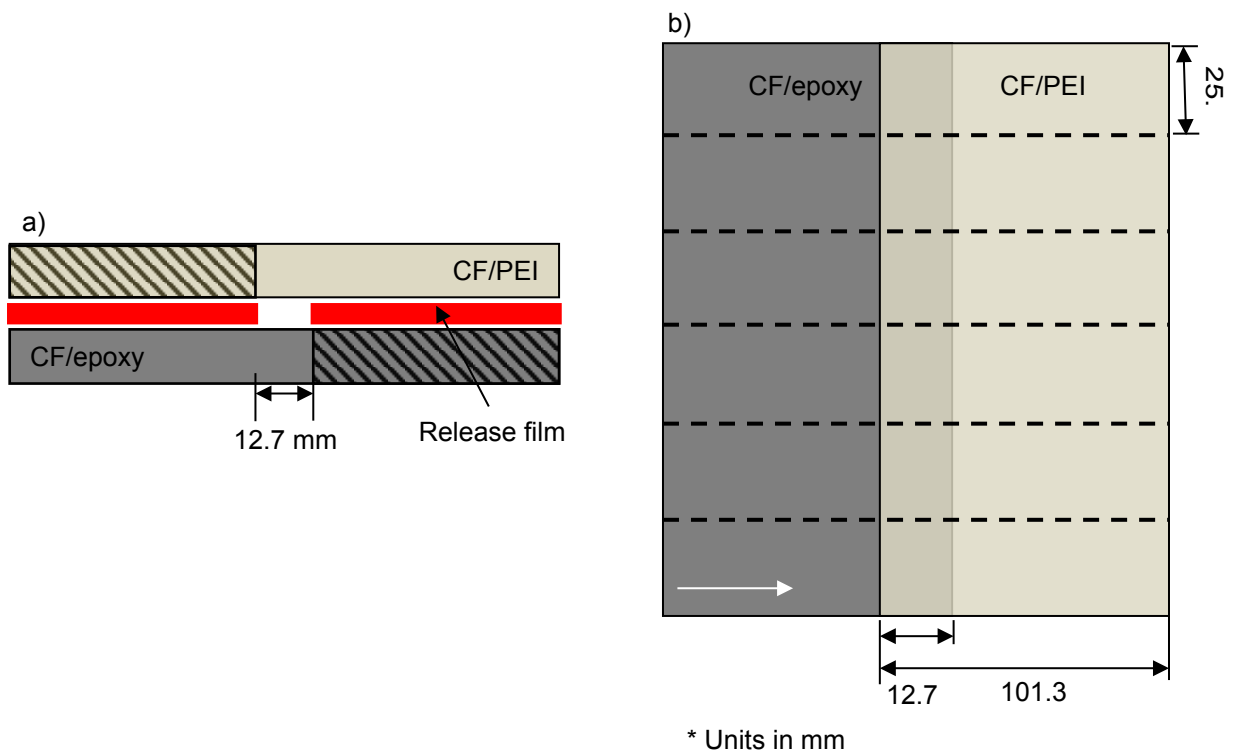


Figure 1: Schematic representations of a) the manufacturing of the reference co-cured samples and b) the location of the cuts, represented by the dash lines. The white arrow points at the 0° fibres of the CF/epoxy adherend and the main apparent orientation of the fibres of the CF/PEI adherend. Dimensions are not to scale.

## 2.2 Welding process

Individual samples were welded with a Rinco Dynamic 3000 ultrasonic welder in a single lap configuration, with the overlap being 12.7 mm long and 25.4 mm wide. The custom-made welding jig shown in Figure 2 was used. A cylindrical sonotrode with a 40 mm diameter was utilised. To ensure minimum heating times, and hence minimum risk of thermal degradation at an acceptable level of dissipated power, the parameters chosen were 1500 N welding force and 86.2  $\mu\text{m}$  peak-to-peak vibration amplitude. These parameters, which are close to the highest within the limits of the machine, result in very short heating times [3]. Solidification force and time were kept constant at 1500 N and 4 s respectively. The duration of the vibration phase was indirectly controlled through either the downward displacement of the sonotrode or the dissipated energy, as it will be explained in more detail in section 3.2. The variation of the power and displacement of the

sonotrode during the vibration phase were provided by the welding machine at the end of the welding process.

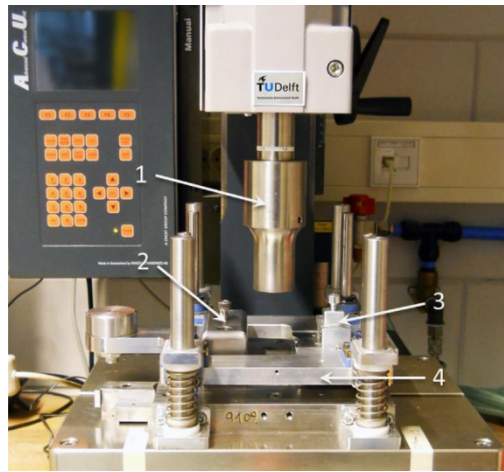
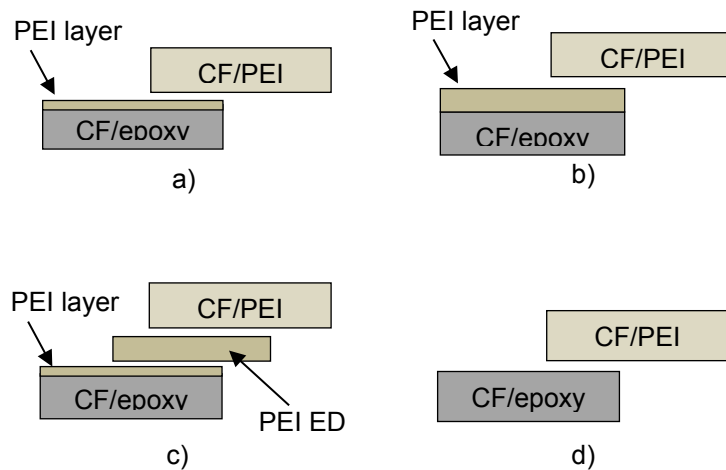


Figure 2: Custom made welding setup. 1: sonotrode, 2: clamp for the lower sample, 3: clamp for the upper sample and 4: sliding platform. [9]

Figure 3 shows the schematics of the different types of joints that were developed in this study. The schematics correspond to (a) joints welded through a 60  $\mu\text{m}$ -thick coupling layer, hereafter referred to as ED-less-60 case, (b) joints welded through a 250  $\mu\text{m}$ -thick coupling layer, hereafter referred to as ED-less-250 case, (c) reference joints welded with a 250  $\mu\text{m}$ -thick loose ED and a 60  $\mu\text{m}$ -thick coupling layer, hereafter referred to as welded reference ED case and (d) co-cured reference joints. **In the reference ED case, the ED was fixed on top of the CF/epoxy adherend with adhesive tape (the size of the ED was slightly bigger than the size of the overlap).**



*Figure 3: Schematic representation of CF/PEI- CF/epoxy/PEI stack for the a) ED-less-60 case, b) ED-less-250 case, c) reference ED case and d) reference co-cured case. Dimensions are not to scale.*

## **2.3 Testing**

Single-lap shear tests were performed in order to assess the mechanical performance of the joints based on the ASTM D 1002 standard. A Zwick 250 kN universal testing machine operating at 1.3 mm/min cross-head speed and under displacement control was used for these tests. The apparent lap shear strength (LSS) of the joints was calculated as the maximum load divided by the overlap area. Five specimens were tested per welding case to determine the average LSS and corresponding standard deviation. Naked-eye observation and scanning electron microscopy (JEOL JSM-7500F Field Emission Scanning Electron Microscope, SEM) were used for fractographic analysis of tested joints. An optical microscope (Zeiss Axiovert 40) together with the SEM were used for cross-sectional analysis of as-welded specimens. Samples for cross-sectional microscopy were embedded in EpoFix resin and subsequently grinded and polished. To observe the epoxy-PEI interphase, polished samples were etched with 1 ml of N-Methyl-2-pyrrolidone (NMP) and then immediately rinsed with ethanol and distilled water to provide a better contrast [5].

## **3. Results**

### **3.1. Baseline study: Interphase between T800s/3911 and PEI materials**

This section aims at i) answering whether an interphase was formed between the T800s/3911 prepreg and the PEI coupling layers, and the T800s/3911 prepreg and the CF/PEI adherend in the co-cured reference joints, after the co-curing process and ii) describing the interphase morphology. **Figure 4a** shows the optical micrograph of an etched CF/epoxy sample with the 60  $\mu\text{m}$  thick PEI coupling layer. A darker grey area can be seen in between the epoxy matrix, which

is a lighter grey colour, and the PEI, which shows scratches that were exposed by the etching process. Note that the spherical particles present in the epoxy resin, with diameters between a few  $\mu\text{m}$  and  $10\ \mu\text{m}$ , are thermoplastic toughening particles present in the T800s/3911 prepreg. A closer look to the circled area (b) in Figure 4a is presented in the SEM image of Figure 4b. In this image is shown that the above-mentioned darker grey area corresponds to the interphase that was formed between the epoxy and PEI materials during the co-curing process. The interphase consists of epoxy spheres dispersed in a PEI-rich matrix, with diameters decreasing towards the PEI coupling layer. Similar interphase morphologies have been seen in previous works, in which PEI was co-cured with a Hexply M18/1 (Hexcel) prepreg [5] or epoxy resins with different formulations [7], [10]–[12]. As explained in those studies, during the co-curing process, the liquid-reactive epoxy system acts as a solvent of the PEI resin. This results in the epoxy monomers diffusing into the glassy PEI and partially dissolving it. Partial dissolution of the PEI polymer allows at the same time for diffusion of the PEI into the liquid epoxy resin. This interdiffusion process between the epoxy and PEI systems stops once the epoxy resin reaches the gelation point. Because of the limited miscibility between the rubbery epoxy and the PEI resins, phase separation occurs. This results in a gradient concentration of the two polymers, hence a gradient interphase between the two materials, with the morphology seen in Figure 4b. The epoxy flow front into the PEI material is also visible in Figure 4b. The area between this flow front and the smallest visible epoxy spheres, with an apparently smooth texture corresponds, most likely, to either an area in which the concentration of the epoxy monomers in the PEI resin was very low, resulting in no phase separation of the two resin systems, or an area with epoxy spheres with a size that was not resolved by the microscope. The thickness of the interphase varies and has a maximum value of around  $25\ \mu\text{m}$ . The same interphase morphology was observed in the co-cured T800s/3911 prepreg and  $250\ \mu\text{m}$ -thick coupling layer.

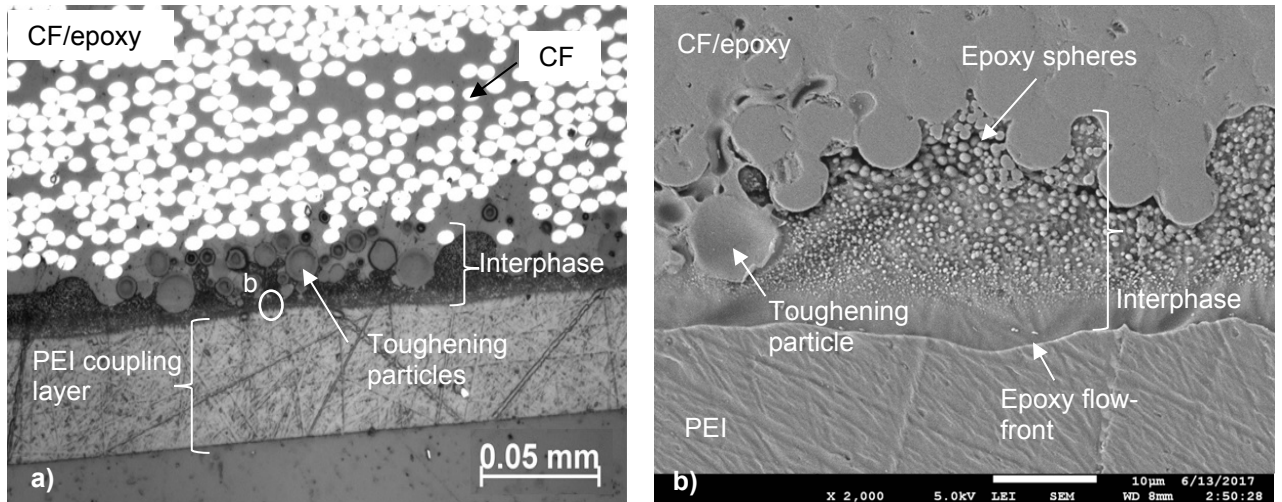


Figure 4: Cross-section images of an etched sample cut from the CF/epoxy/PEI laminate obtained via a) optical microscopy, in which the interphase can be seen as a dark grey area between the epoxy and the PEI resin (both with lighter grey colours) and b) SEM, which shows an interphase with a gradient morphology.

Figure 5a presents the optical micrograph of an etched reference co-cured sample. As shown in the image, the interphase is not visible with optical microscopy, therefore SEM analysis is necessary to examine whether an interphase was formed. The SEM image in Figure 5b shows the existence of an interphase similar to the one formed in the CF/epoxy/PEI laminates, with epoxy spheres dispersed in the PEI-rich matrix resin, indication of inter-diffusion between the epoxy and PEI matrices. However, the two interphases have a different maximum thickness, with the interphase of the co-cured reference sample being almost 40 µm, whereas for the interphase formed with the neat PEI film the thickness is 25 µm. Epoxy spheres can be found deeper into the CF/epoxy laminate, in the interphase of the co-cured reference sample. The density of the epoxy spheres in the PEI resin also seems to be higher for the co-cured reference samples. The reason why the interphase formed between the CF/epoxy and CF/PEI prepregs shows some differences, might be a different PEI grade between the 60 microns SABIC PEI coupling layer and the Cetex® CF/PEI prepreg of the TPC adherend (reference co-cured case).

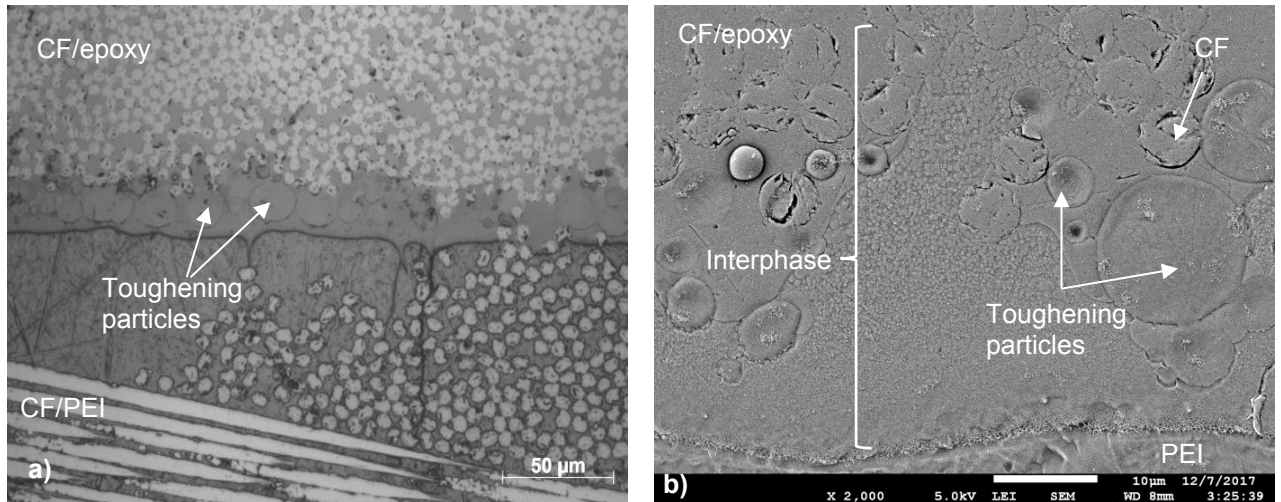


Figure 5: Cross-section images of etched co-cured reference sample obtained via a) the optical microscope, in which no signs of a formed interphase can be seen, and b) the SEM, which shows that an interphase is formed with epoxy spheres embedded in the PEI resin.

### 3.2. Effect of the different welding cases on the welding process

Figure 6 illustrates the representative power and displacement curves plotted versus time of samples welded according to the three welding cases shown in Figure 3, namely the ED-less-60, ED-less-250 and the reference ED cases. The curves correspond to displacement-controlled process in which the downward movement of the sonotrode reached the total thickness of the coupling layer, for the ED-less cases, or the thickness of the ED for the reference ED case. Two power peaks can be found in the power curves of all cases. The displacement stays at around zero during the first power peak. The time during which the displacement is zero, however, differs per case. This stage lasts approximately 250 ms longer for the ED-less cases, as compared to the reference ED case. The displacement starts increasing when the power starts increasing after the first peak. The rate at which the displacement increases is the fastest for the reference ED case and the slowest for the ED-less-60 case.

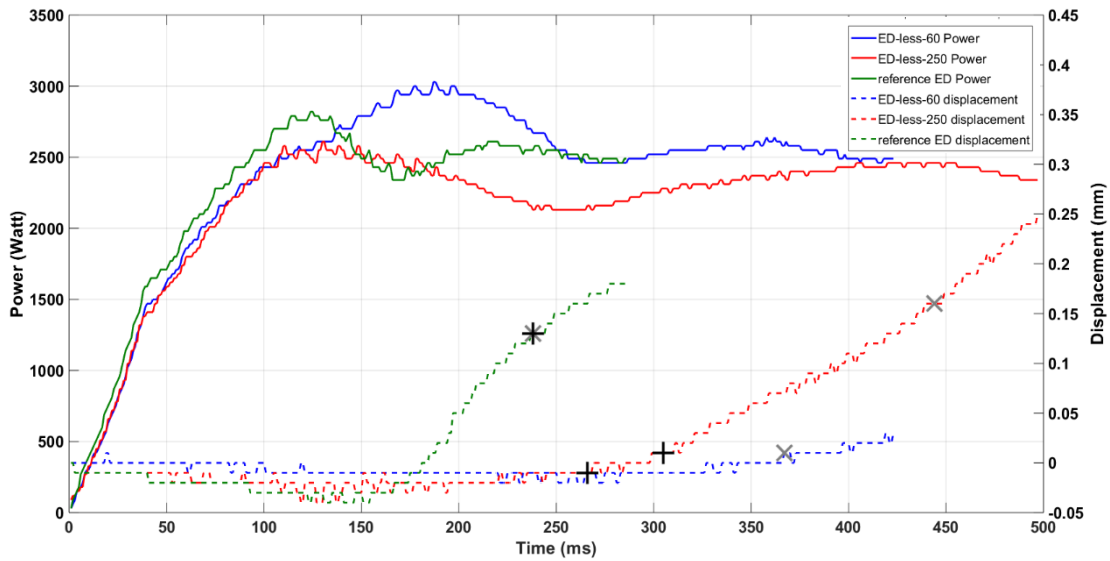


Figure 6: Representative power (solid line) and displacement (dotted line) curves of samples welded according to the three different welding cases. The grey “x” points indicate the initial expected optimum displacement values, according to the procedure defined for ultrasonic welding of TPCs with a loose ED [13]. The black “+” points indicate the actual optimum displacement values used for the welding.

In welding of TPCs the power and displacement curves are used to determine the optimum duration of the vibration phase [13]. It is shown in [13] that stopping the welding process close to when the second power peak occurs, results in welds with the highest strength. In the reference ED case, samples welded in displacement-control mode with a target displacement of 0.13 mm (which corresponds to the second power peak) featured, upon mechanical testing, no signs of overheating and satisfactory strength values, as it will be shown in section 3.4.2. In the ED-less-60 case, the second power peak corresponded to zero displacement and hence an energy-controlled process had to be used. Through a trial-and-error process, it was found that welding between 500 J (which corresponds to the second increase in power and is indicated with the black “+” point in Figure 6) and 700 J (which corresponds to the second power peak, indicated with the grey “x” point), resulted in welds with similar strength. All of them featured unwelded areas and degradation signs of the PEI resin, as it will be shown in section 3.4.2. Hence, to minimise the thermal effects, 500 J was chosen as the optimum energy. In the ED-less-250 case, samples welded with a target displacement of 0.15 mm (expected optimum displacement, indicated with

the grey “x” point in Figure 6) featured, upon testing, fibre distortion in the CF/PEI adherend, potentially due to excessive PEI resin flow [14]. A trial-and-error process had to be followed, in order to find more adequate welding conditions. It was found that the welds with the highest mechanical performance and least fibre distortion were achieved for an energy value of 600 J (black “+” point in Figure 6) . Note that energy-controlled welding had to be used since the vibration had to be stopped close to the onset of the downward displacement of the sonotrode, therefore at approximately zero displacement, as seen in Figure 6.

### **3.3 Effect of the welding process on the welding stack integrity**

#### **3.3.1 Optical microscopy**

In order to evaluate the effect of the welding process on the integrity of the welding stack, i.e., the adherends, the coupling layer and the interphase, cross-sectional analysis of as-welded samples was performed. The main focus points of this analysis were (i) to determine the thickness of the weld line, since it is an indication of how much neat resin has flowed and it can also have an influence on the mechanical performance of the joints, and (ii) to identify thermal degradation signs in the form of porosity. Note that the weld line is defined in this study as the PEI-rich region between the fibre bundles of the CF/epoxy and CF/PEI adherends. Figure 7 shows the optical micrograph of the cross-section of an ED-less-60 sample. Porosity within the weldline and the first ply of the CF/PEI adherend can be observed, as seen in the circled areas in [Figure 7](#). The weldline has a thickness of around 70  $\mu\text{m}$ . Figure 8 presents the cross-sectional optical micrograph of an ED-less-250 sample. Some porosity can be seen near the edge of the overlap and close to the CF/PEI adherend. The thickness of the weldline is approximately 200  $\mu\text{m}$ .

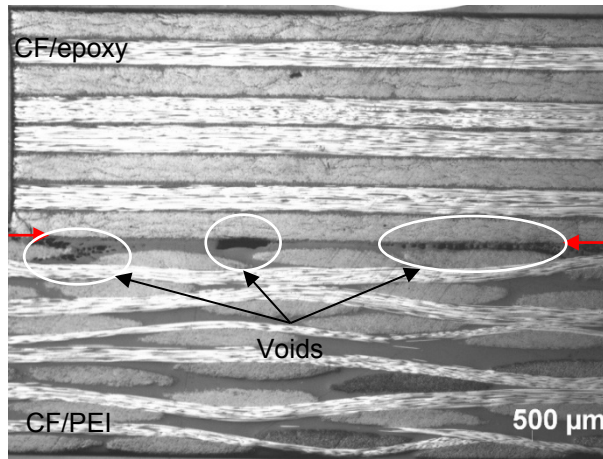


Figure 1: Cross-sectional micrograph close to the edge of an ED-less-60 sample welded at 500 J. Porosity can be seen within the weld line. Red arrows indicate the weld line.

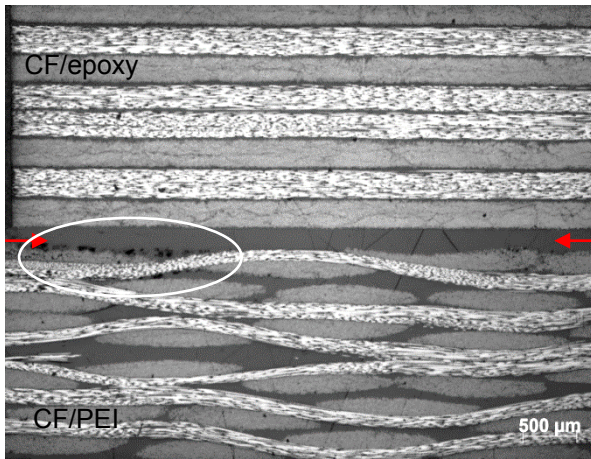
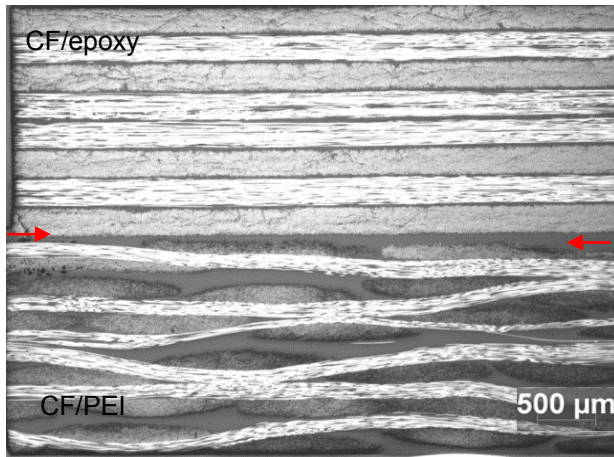


Figure 8: Cross-sectional micrograph close to the edge of an ED-less-250 case sample welded at 600 J. A thick weld line and porosity in the weld line can be observed. Red arrows indicate the weld line.

Figure 9 presents an optical micrograph of a reference ED sample. No signs of porosity within the weld line and in the two composite adherends can be found. The thickness of the weld line is approximately 110  $\mu\text{m}$  and it seems to be similar to the ones typically observed in literature for ultrasonically welded TPC joints [15,16]. The thickness of the weld line decreases towards the edges, where squeeze out of resin occurs.



*Figure 9: Cross-sectional micrograph close to the edge of a reference ED sample welded at 0.13 mm displacement revealing no porosity in the weld line. Red arrows indicate the weld line.*

### **3.3.2 Scanning electron microscopy**

During the welding process, it is likely that the coupling layer will soften and flow, especially in the ED-less cases, in which the coupling layer is expected to act as an integrated ED. Hence, it could happen that flow of the coupling layer close to the interphase altered the initial interphase morphology between the epoxy matrix and the PEI film. In order to assess whether the welding process affected the interphase, SEM analysis of the cross-sections presented in the previous section was performed. Figure 10 depicts the SEM images of as-welded specimens for each welding case. It is observed that for all cases the post-welded interphase has the same morphology as the original one.

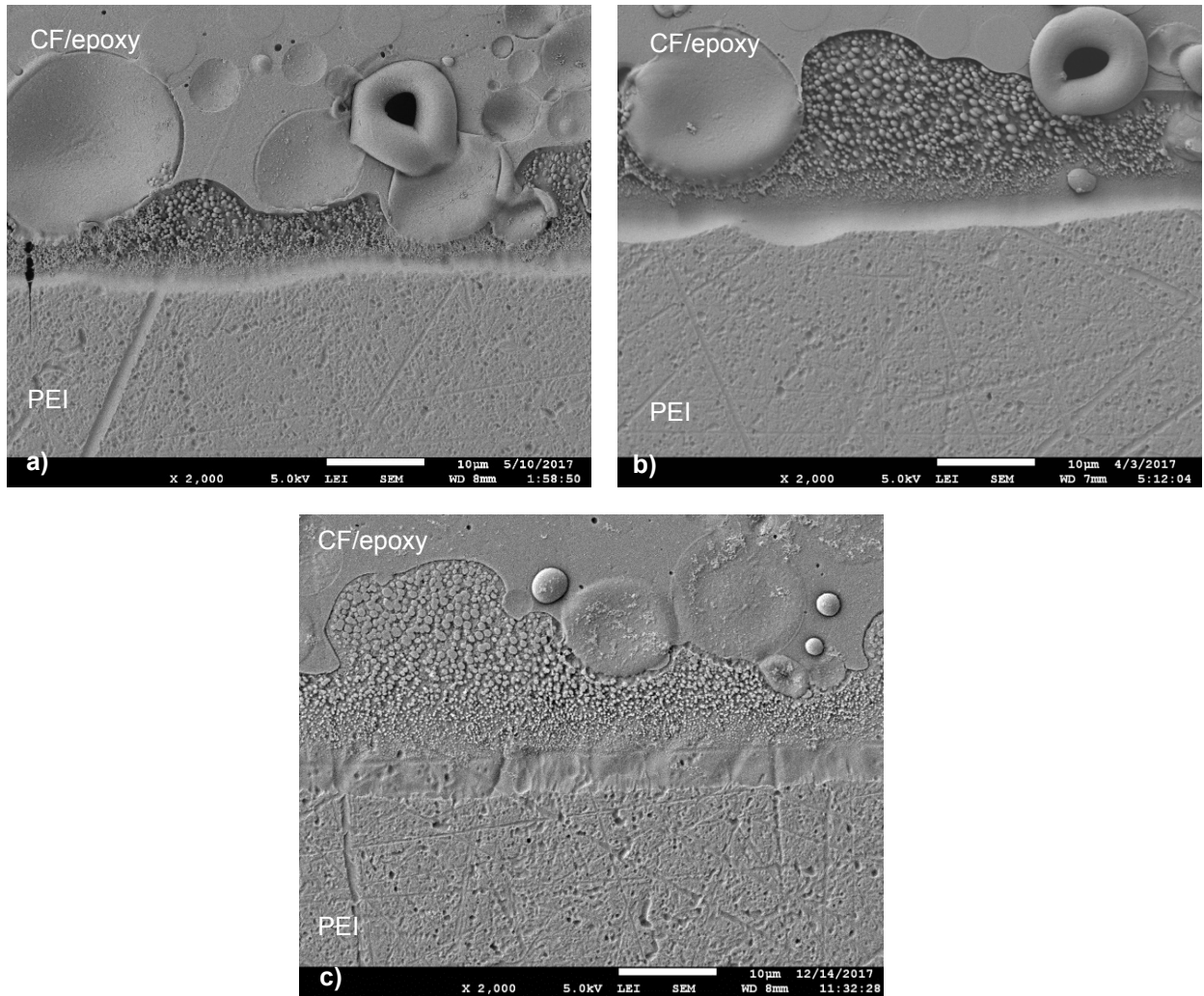


Figure 10: SEM images of as-welded specimens for the (a) ED-less-60, (b) ED-less-250 and (c) reference ED cases. The interphase morphology is the same for all welding cases.

### 3.4. Mechanical performance and failure analysis of welded and reference joints

#### 3.4.1 Single-lap shear tests

The results of the single-lap shear tests are illustrated in Figure 11. The ED-less-60 samples have a LSS of  $17.3 \pm 4.5$  MPa (average  $\pm$  standard deviation) with a 26% coefficient of variation (cov), while the ED-less-250 case samples have a LSS of  $29.3 \pm 3.2$  MPa (11% cov). The LSS of the reference ED samples is the highest with the lowest scatter amongst the welded samples, i.e.  $37.7 \pm 1.6$  MPa (4% cov). The co-cured samples exhibit a LSS of  $34.7 \pm 1.4$  MPa (4% cov).

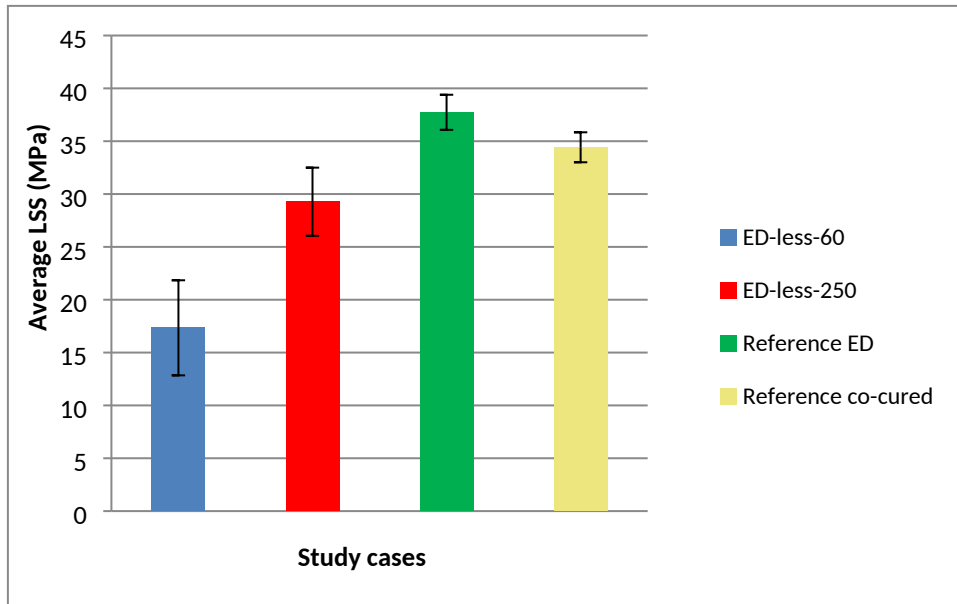


Figure 11: LSS values of the reference and welded samples with corresponding standard deviation.

### 3.4.2 Fractography

Fractographic analysis was used in order to further evaluate the mechanical performance of the joints. Figure 12 shows three typical fracture surfaces of ED-less-60 samples after testing. Note that they were all welded with the same welding parameter, i.e. 500 J. Unwelded areas covering a significant part of the overlap can be seen in all samples. The amount and location of the unwelded areas are inconsistent per sample and most of the welded areas display discoloured resin that can potentially result from thermal degradation. The lack of exposed fibres indicates that failure occurred entirely in the neat PEI resin, most probably in the coupling layer. The sample exhibiting the highest strength and largest welded areas is chosen for further microscopic analysis (the left most sample in Figure 12), the results of which are presented in Figure 13a.



*Figure 12: Fracture surfaces obtained from ED-less-60 samples welded at 500 J. The white lines indicate the unwelded areas.*

Figure 13b depicts a SEM image of the area circled in Figure 13a. Numerous voids and flakes can be seen in the PEI resin, however it is unclear whether they were coming from the coupling layer or the PEI matrix in the CF/PEI adherend. Such features are mostly linked to thermal degradation of the PEI resin, as presented in the work of Palardy and Villegas [15]. A closer examination of the area (c) indicated in Figure 13b, reveals exposed epoxy spheres which are part of the interphase, and toughening particles, which are indications of interphase failure and possibly epoxy matrix failure (Figure 13c).

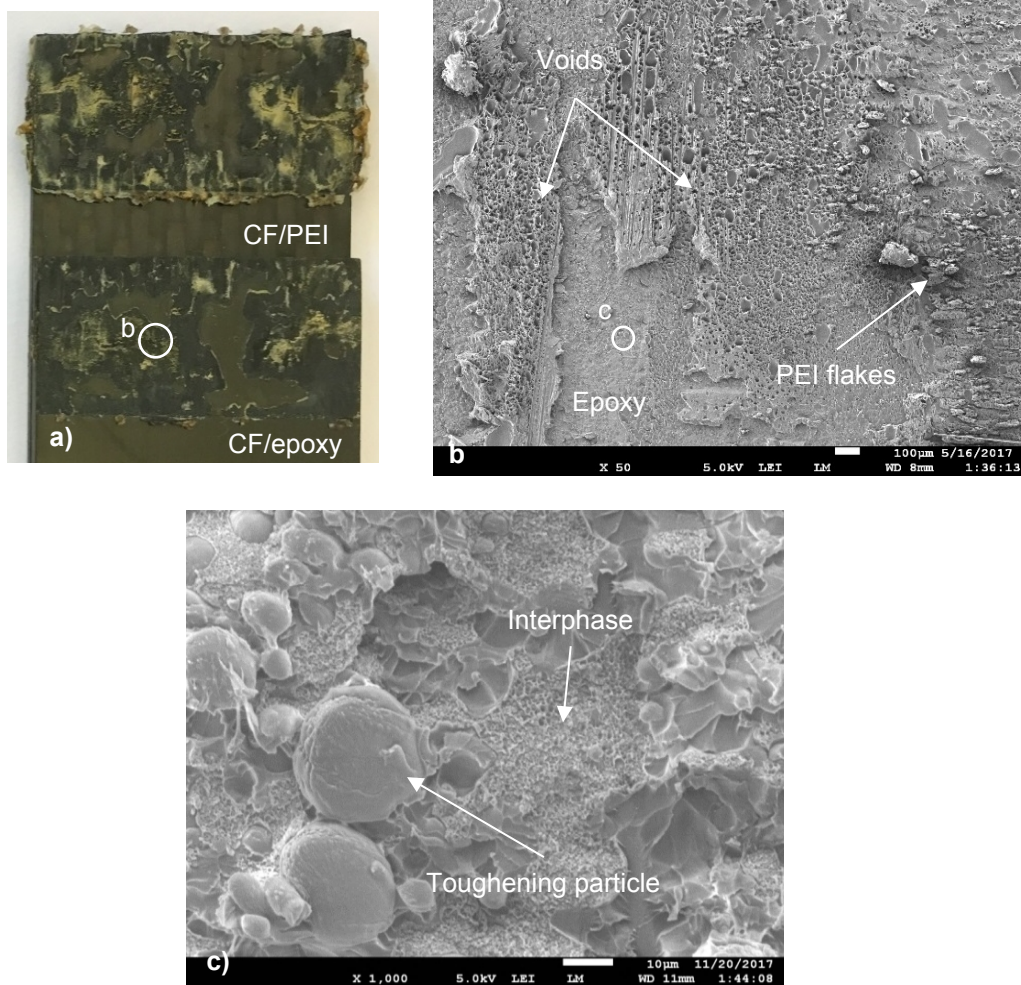


Figure 13: (a) Representative fracture surfaces of an ED-less-60 case sample showing large unwelded areas and signs of thermal degradation of the PEI resin. (b) SEM image corresponding to the circled area in (a), depicting voids in the PEI resin and PEI resin flakes, both features associated with thermal degradation and (c) is a detailed SEM image showing failure in the interphase

Figure 14 shows three typical ED-less-250 fracture surfaces of samples welded with the same parameters. The fracture surfaces appear more uniform than in the ED-less-60 case and for most samples no unwelded areas are present. The failure mechanism is characterized by first ply failure in the CF/PEI adherend. In some samples, however, like the first and third samples in Figure 14, discoloured PEI resin is seen, similar to what was observed in the ED-less-60 samples. For further analysis the sample exhibiting the highest strength and largest welded area (left most sample in Figure 14) is chosen and is illustrated in Figure 15a.



*Figure 14: Fracture surfaces obtained from ED-less-250 samples welded at 600 J. Unwelded areas are indicated by the white lines. White arrows indicate locations with discoloured PEI resin.*

Figure 15b shows a SEM micrograph of the circled area (b) in Figure 16a and displays slightly deformed fibre bundles in the CF/PEI adherend. In Figure 15c, failure in the CF/epoxy adherend is also partially seen, characterized by mostly matrix failure and only a few exposed fibres or fibre imprints. This failure however is not the predominant type of failure and it is only found at one of the edges of the overlap on the CF/epoxy adherend, as indicated by the circled area (c) in Figure 15a. Numerous voids on the fracture surface of the CF/PEI adherend can be seen at the abovementioned location, indicating thermal degradation of the PEI resin. Degradation signs in the form of voids and resin flakes are also found in an area in the middle of the overlap (region (d) in Figure 15a), depicted in Figure 15d.

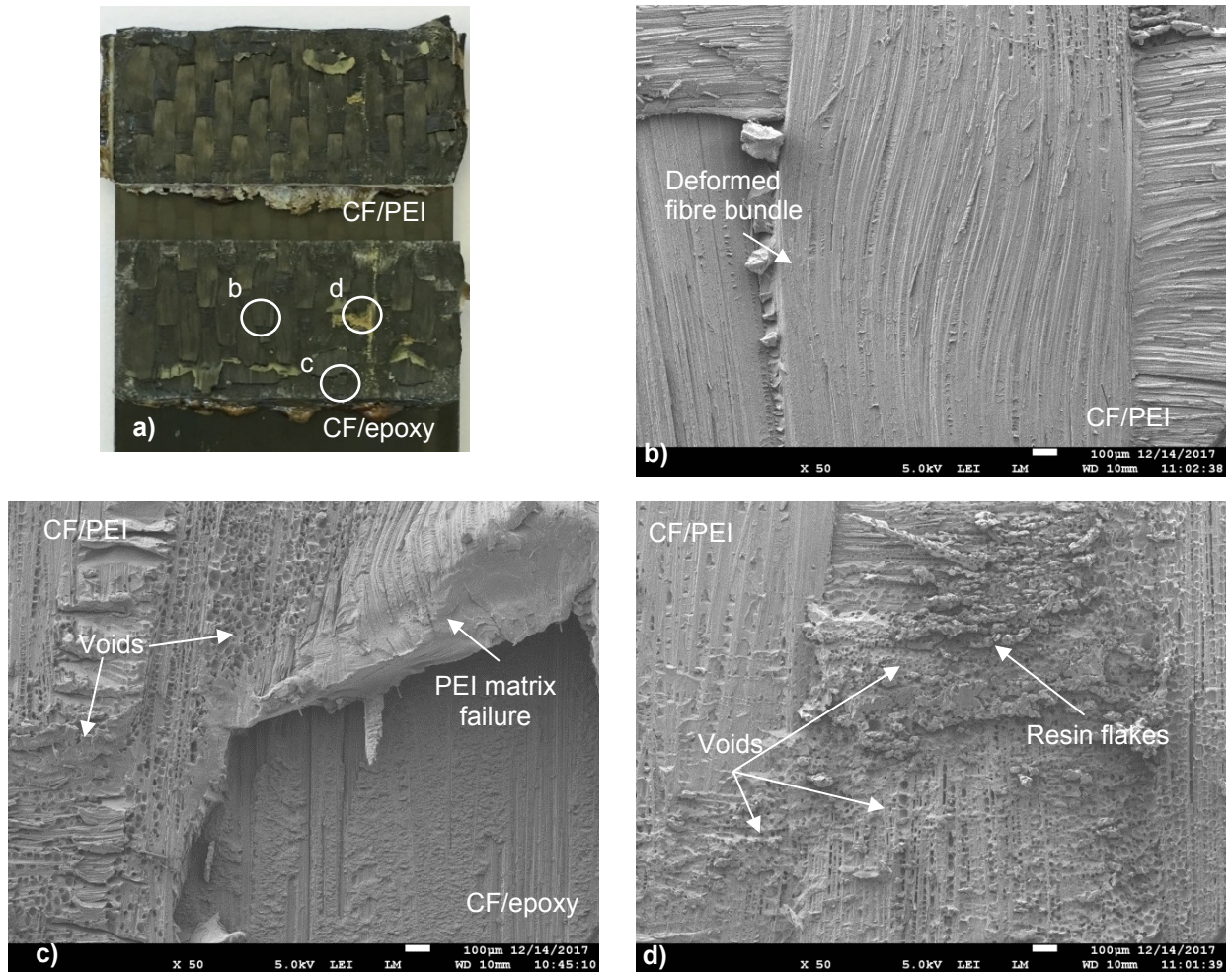


Figure 15: (a) Representative fracture surfaces of an ED-less-250 sample showing failure mostly in the CF/PEI adherend, with only partial failure in the CF/epoxy adherend and (b), (c), (d) are SEM images corresponding to the circled areas in (a), showing (b) deformed fibre bundles (c) degradation signs in the form of voids close to the edge of the overlap and (d) voids and resin flakes in the middle of the overlap.

Figure 16a shows the representative fracture surfaces of reference ED samples, exhibiting a fully welded overlap. First-ply failure in the CF/PEI adherend is the dominant failure mechanism, indicated by the broken fibre bundles of the CF/PEI adherend that are found on the CF/epoxy adherend. Failure in the CF/epoxy adherend is limited and only some exposed fibres are seen on the fracture surfaces. Such observations are supported by SEM inspection pertaining to the CF/epoxy adherend, as the micrograph in Figure 16b illustrates. The micrograph also shows some epoxy-rich areas. Closer inspection of the epoxy-rich areas reveals failure both in the epoxy

resin and the interphase, presented in Figure 16c. However, such failure type is found only at a few locations in the overlap. No thermal degradation signs of the PEI resin can be observed throughout the fracture surfaces.

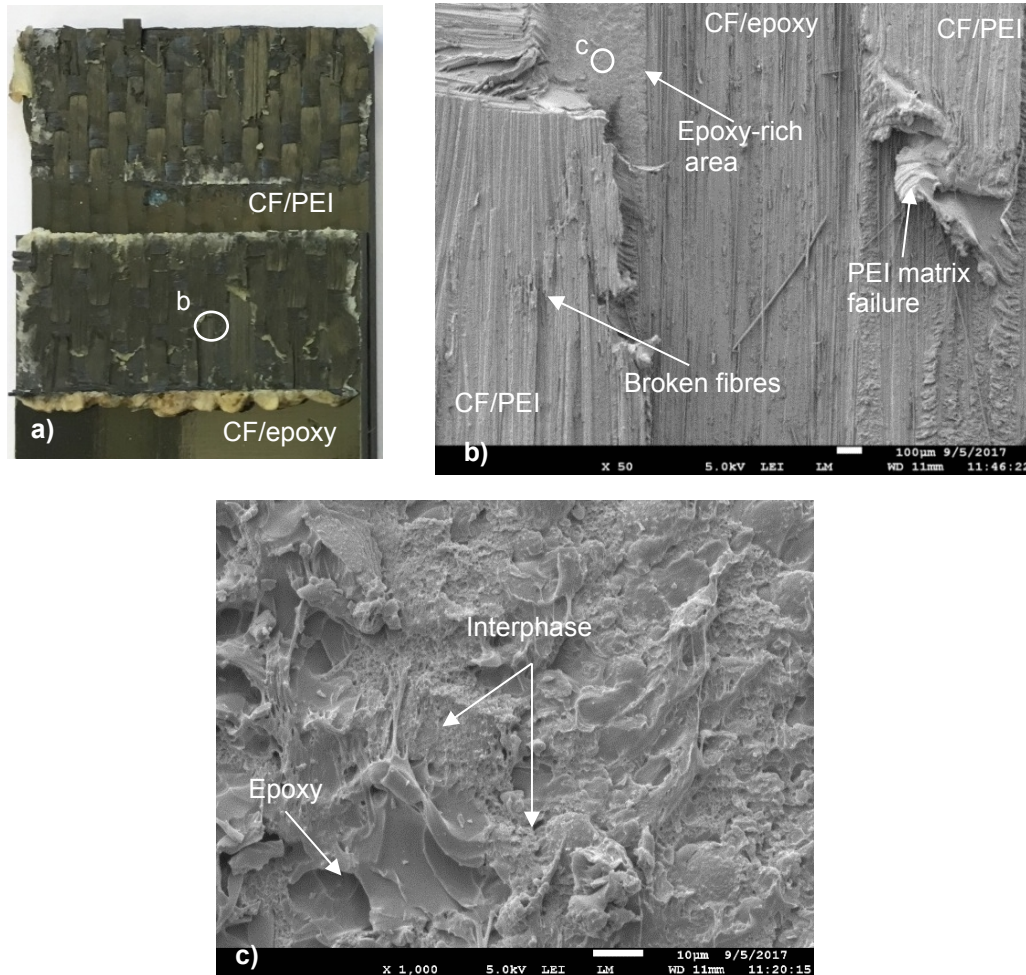


Figure 16: (a) Representative fracture surfaces of a reference ED sample welded at 0.13 mm displacement, showing failure mostly in the CF/PEI adherend, with only partial failure in the CF/epoxy adherend. (b) SEM image corresponding to the circled area in (a), showing broken CF/PEI bundles and exposed fibres in the CF/epoxy adherend, (c) SEM image showing failure in the epoxy and interphase.

Figure 17a illustrates representative fracture surfaces for the reference co-cured case. Naked-eye inspection reveals first ply failure in both CF/epoxy and CF/PEI adherends. The failure is characterized by exposed fibres and resin rich areas. Closer inspection of the circled area (b) in

Figure 17a by means of SEM (Figure 17b), shows matrix failure in the CF/PEI adherend, exposed fibres from the CF/epoxy adherend, as well as epoxy resin rich areas. Figure 17c depicts a closer view of the circled area (c) in Figure 17b, in which epoxy resin is fractured, demonstrating matrix failure, and what seem to be epoxy spheres from the interphase are exposed, linked to interphase failure.

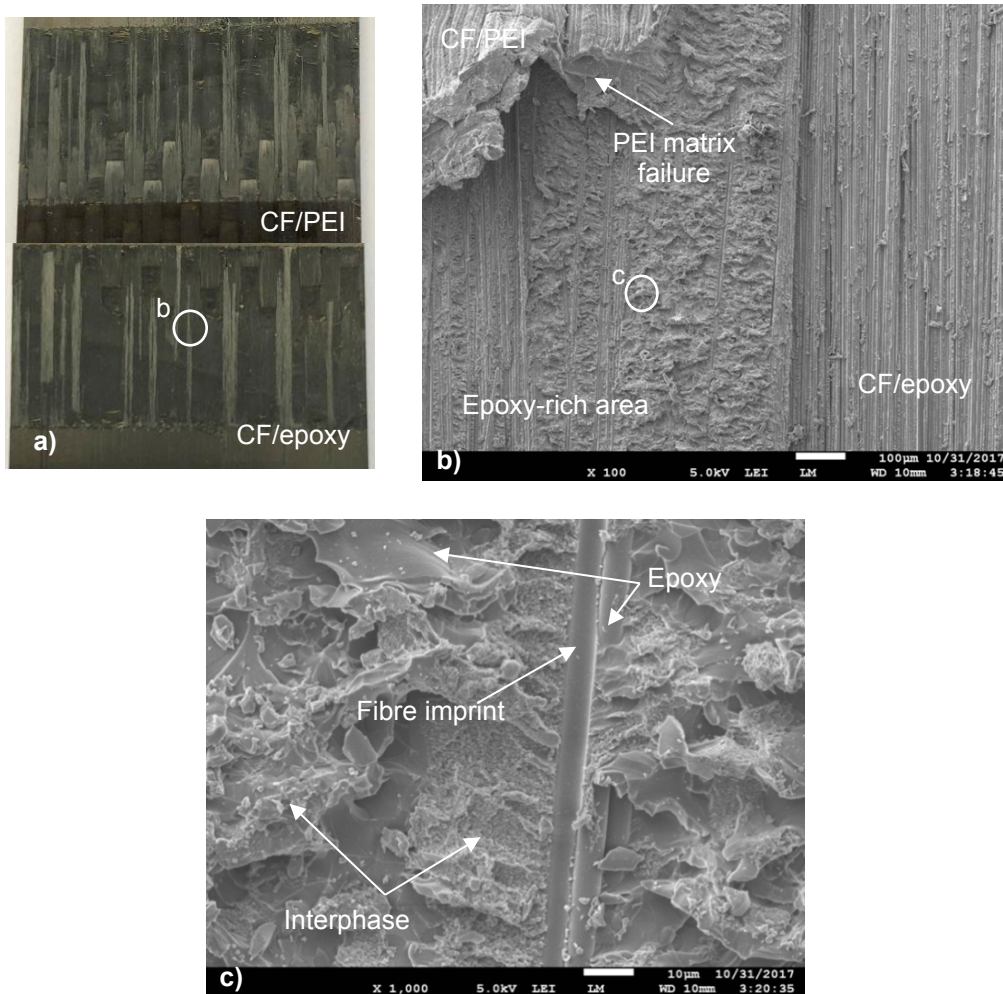


Figure 17: (a) Representative fracture surfaces of a reference co-cured sample, showing failure in the two composites adherends characterised by exposed fibers and resin failure. (b) SEM image corresponding in the circled area in (a), matrix failure in the CF/PEI adherend, exposed fibres in the CF/epoxy adherend and matrix failure. (c) A more detailed SEM image showing failure in the interphase and epoxy matrix.

#### 4. Discussion

The findings presented in the Results section show that welding of dissimilar composite materials without a loose ED can have a large effect on the quality of the welds, especially when a thin coupling layer is used. The ED-less-60 samples yielded the lowest strength of  $17.3 \pm 4.5$  MPa. The ED-less-250 samples resulted in a higher LSS ( $29.3 \pm 3.2$  MPa) as compared to the ED-less-60 samples, but still lower than the reference cases. The reference ED samples yielded the highest LSS, i.e.  $37.7 \pm 1.6$  MPa, and the reference co-cured samples exhibited an average strength of  $34.7 \pm 1.4$  MPa.

Comparing the ED-less-60 samples with the reference ED samples, it is obvious that the lower LSS of the former is attributed to the large unwelded areas and the degradation of the PEI resin that were found on all samples. On the contrary, the reference ED samples featured fully welded overlaps and no signs of thermal degradation of the PEI resin. **The unwelded areas in the ED-less-60 samples can be attributed to firstly limited contact areas and secondly the lack of resin flow during the welding process**, evident by the fact that the final thickness of the weld line was similar to the original thickness of the 60  $\mu\text{m}$ -thick coupling layer. During welding, frictional heating was initiated in areas where the two adherends were in good contact with each other, for the ED-less-60 case, or with the ED, for the reference ED case. The locations at which a good initial contact is established, is normally random per sample since it depends on the surface quality and the thickness variations of the ED and the adherends. **It is expected that the initial contact areas are larger in the reference ED case as opposed to the ED-less-60 case. The ED is relatively thin and has the ability to deform and therefore conform to the surface irregularities. On the other hand, the coupling layer is fixed on the much stiffer adherend, hence deformation of the coupling layer is more limited than the ED. Regarding the resin flow**, in the reference ED case, once the  $T_g$  was reached, the PEI resin in those areas flowed under the pressure applied by the sonotrode. Thus, the downward movement of the sonotrode and the flow of the resin in the initial contact areas, resulted in a good overall contact in the rest of the overlap, ensuring fully welded areas. However, in the ED-less-60 case, the welding process was stopped before any downward movement of the sonotrode occurred. Hence, only the initial contact areas were being heated up.

This resulted in the large and non-uniformly distributed unwelded areas. Regarding the degradation signs found in the ED-less-60 samples, they are most likely caused by (i) the lack of resin flow, (ii) limited frictional heating when solely the coupling layer is used, as compared to when the ED is used and (iii) the small thickness of the coupling layer. Firstly, lack of resin flow in the ED-less-60 case caused the resin at the initial contact areas to be continuously heated up and most likely eventually overheated. Secondly, in welding of the reference ED case, friction was generated between two sides of the ED and the adherends in contact, most probably securing that the ED will reach the  $T_g$  faster than the adherends. However, in the ED-less-60 case, only one side of the coupling layer was subjected to frictional heating. It is possible that both coupling layer and CF/PEI adherend were heating up at the same rate, exposing them to high temperatures for a longer time in comparison with the reference ED case. Lastly, the small thickness of the coupling layer might also have contributed to overheating of the CF/PEI adherend. As seen in the research by Palardy and Villegas [15], a 60  $\mu\text{m}$ -thick ED was unable to generate preferential heat at the interface, causing overheating of the CF/PEI adherends.

Increasing the thickness of the coupling layer to 250  $\mu\text{m}$  resulted in welds with a higher strength when compared to the ED-less-60 case, probably because of the fully welded overlaps. The final thickness of the weld line of the ED-less-250 samples was 200  $\mu\text{m}$ , indicating that flow of the PEI resin occurred during welding. Note that since the vibration phase was stopped when the displacement of the sonotrode was zero, flow of the PEI resin most likely occurred during the solidification phase. This allowed for the whole overlap to be welded in most samples. However, the limited frictional heating on the coupling layer caused overheating of the coupling layer and CF/PEI adherend, resulting subsequently in a lower strength when compared to the reference ED samples. Moreover, the thicker weld line of the ED-less-250 samples (i.e. 200  $\mu\text{m}$ ) as compared to the reference ED samples (i.e. 110  $\mu\text{m}$ ), might have resulted in higher peel stresses due to secondary bending during the SLS test, hence a lower LSS for the ED-less-250 case [16].

As already discussed in the previous paragraphs, there were clear indications of thermally degraded PEI resin after the welding process. However, no visible signs of degraded epoxy resin (in the form of voids) could be found in any of the as-welded samples and, the interphase

appeared to be intact after welding. Still, when the 60  $\mu\text{m}$ -thick coupling layer was used, either by itself or with the addition of an ED, failure occurred partially in the epoxy resin and interphase. However, when the 250  $\mu\text{m}$ -thick coupling layer was used failure occurred almost entirely in the CF/PEI adherend. Failure in the epoxy resin and interphase could be a sign of thermal degradation of the epoxy resin, even though no porosity or altered features of the epoxy resin could be seen with the microscopes used in this study. However, this type of failure also occurred in the reference co-cured samples, in which it is certain that no thermal degradation occurred. Therefore, failure in the CF/epoxy adherend might be possibly attributed to the thin weld line or bond line of the ED-less-60 (i.e. 70  $\mu\text{m}$ ) and reference co-cured samples (practically zero), which can potentially have an effect on the stresses developed during the SLS test. Nevertheless, further research is needed to determine whether the epoxy resin is degraded during welding.

## Conclusions

In this paper experimental assessment of the feasibility of ED-less ultrasonic welding of CF/epoxy to CF/PEI composites was presented. Two welding cases were considered: welding solely with (i) a 60  $\mu\text{m}$ -thick (ED-less-60 case) and (ii) a 250  $\mu\text{m}$ -thick (ED-less-250 case) co-cured coupling layer. These welding cases were then compared to two reference cases, a) welding with a 250  $\mu\text{m}$ -thick loose ED and a 60  $\mu\text{m}$ -thick coupling layer (reference ED case) and b) co-cured CF/epoxy and CF/PEI samples, without a coupling layer (reference co-cured case). The analysis of the results led to the following conclusions:

- Welding with solely the coupling layer probably caused limited frictional heating, which in return resulted in overheating of the CF/PEI adherend and/or coupling layer. Overheating of the CF/PEI adherend was indicated by PEI resin flakes and voids, features that have been associated in previous research with thermal degradation of the PEI resin.
- For the ED-less-60 case, absence of resin flow during welding resulted in large unwelded areas. The only areas that were heated and welded where the initial contact areas where the coupling layer and the CF/PEI adherend were in intimate contact. On the other hand, flow of

the coupling layer during the welding process of the ED-less-250 case resulted in better contact between the coupling layer and the adherends and therefore fully welded overlaps.

- For the reasons mentioned above, the ED-less-60 samples yielded a lower LSS of  $17.3 \pm 4.5$  MPa when compared to the ED-less-250 samples that provided a LSS of  $29.3 \pm 3.2$  MPa. The reference samples yielded higher LSS values, possibly because of the lack of thermal degradation signs of the PEI resin. The reference ED samples and reference co-cured samples exhibited a  $37.7 \pm 1.6$  MPa and  $34.7 \pm 1.4$  MPa LSS accordingly.
- Failure in the CF/epoxy for the welded joints in which a 60  $\mu$ m-thick coupling layer was used, might indicate some type of thermal degradation of the epoxy resin not traceable through SEM, as no porosity could be found in the epoxy resin. Further research on whether the epoxy resin is affected by the welding process is needed.

### **Acknowledgements**

This research is part of the European project EFFICOMP that focuses on efficient manufacturing of composite parts. The EFFICOMP project received funding from the European Union Horizon 2020 research and innovation program under grant agreement No 690802.

The authors would like to acknowledge the two anonymous reviewers, whose feedback helped to further improve this paper.

### **References**

- [1] Ageorges C, Ye L, Hou M. Advances in fusion bonding techniques for joining thermoplastics materials composites: a review. *Compos Part A Appl Sci Manuf* 2001;32:839–57.
- [2] da Costa AP, Botelho EC, Costa ML, Narita NE, Tarpani JR. A review of welding technologies for thermoplastic composites in aerospace applications. *J Aerosp Technol Manag* 2012;4:255–65.

- [3] Villegas IF, Rubio PV. On avoiding thermal degradation during welding of high-performance thermoplastic composites to thermoset composites. *Compos Part A Appl Sci Manuf* 2015;77:172–80.
- [4] Schieler O, Beier U. Induction welding of hybrid thermoplastic-thermoset composite parts. *Int J Appl Sci Technol* 2016;9:27–36.
- [5] Villegas IF, van Moorleghe R. Ultrasonic welding of carbon/epoxy and carbon/PEEK composites through a PEI thermoplastic coupling layer. *Compos Part A Appl Sci Manuf* 2018;109:75–83.
- [6] Don RC, Gillespie Jr. JW, McKnight SH. Bonding techniques for high performance thermoplastic compositions. US5643390A, 1997.
- [7] Lestriez B, Chapel J-P, Gérard J-F. Gradient interphase between reactive epoxy and glassy thermoplastic from dissolution process, reaction kinetics, and phase separation thermodynamics. *Macromolecules* 2001;34:1204–13.
- [8] Zhang Z, Wang X, Luo Y, Zhang Z, Wang L. Study on heating process of ultrasonic welding for thermoplastics. *J Thermoplast Compos Mater* 2010;23:647–64.
- [9] Deng S, Djukic L, Paton R, Ye L. Thermoplastic-epoxy interactions and their potential applications in joining composite structures - A review. *Compos Part A Appl Sci Manuf* 2015;68:121–32.
- [10] Vandi LJ, Hou M, Veidt M, Truss R, Heitzmann M, Paton R. Interface diffusion and morphology of aerospace grade epoxy co-cured with thermoplastic polymers. 28th Int. Congr. Aeronaut. Sci., 2012, p. 1–9.
- [11] Bonnet A, Pascault JP, Sautereau H, Taha M. Epoxy– diamine thermoset/thermoplastic blends. 1. Rates of reactions before and after phase separation. *Macromolecules* 1999;32:8517–23.
- [12] Wang M, Yu Y, Wu X, Li S. Polymerization induced phase separation in poly (ether

- imide)-modified epoxy resin cured with imidazole. *Polymer (Guildf)* 2004;45:1253–9.
- [13] Villegas IF. Strength development versus process data in ultrasonic welding of thermoplastic composites with flat energy directors and its application to the definition of optimum processing parameters. *Compos Part A Appl Sci Manuf* 2014;65:27–37.
- [14] Villegas IF. In situ monitoring of ultrasonic welding of thermoplastic composites through power and displacement data. *J Thermoplast Compos Mater* 2015;28:66–85.
- [15] Palardy G, Villegas IF. On the effect of flat energy directors thickness on heat generation during ultrasonic welding of thermoplastic composites. *Compos Interfaces* 2016;24:203–14.
- [16] Gleich DM, Tooren MJL Van, Beukers A. Analysis and evaluation of bondline thickness effects on failure load in adhesively bonded structures. *J Adhes Sci Technol* 2001;15:1091–101.